RSC Advances

PAPER

View Article Online
View Journal | View Issue

Cite this: *RSC Adv.*, 2014, **4**, 63085

Estimation of electrical parameters inside nanofiltration membranes in various electrolyte solutions by dielectric spectroscopy analysis†

Kongshuang Zhao,* Qing Lu and Wenjuan Su

Received 1st November 2014
Accepted 6th November 2014

DOI: 10.1039/c4ra13598a

www.rsc.org/advances

This work reports the dielectric analysis of three kinds of nanofiltration membranes (NF90, NF- and NF270) in eight electrolyte solutions. The high-frequency relaxation was analyzed theoretically and the relative permittivity and conductivity of the wet-membranes were calculated. Porosity of these membranes and ion solvation energy barrier were calculated using the relative permittivity of the wet-membrane. By combining the conductivity ratio of membrane and solution, κ_m/κ_w, with the TMS model, the volumetric charge density of the membranes was estimated. The concentration expressions of co- and counter-ions in the membranes were deduced based on the Donnan exclusion theory. The wet membrane's relative permittivity rather than the dry one was used in all of the calculations, so the results are very close to the practical separation process. Furthermore, the influencing factors on the ion permeability for three types of NF membranes were discussed by considering the ion concentrations inside the membranes, ion solvation energy barrier and the surface charge density on the pore-wall.

1. Introduction

Dielectric spectroscopy is a particularly insightful method because it can monitor relaxation processes of various systems in a non-invasive way, especially heterogeneous systems including membrane–solution. In our previous paper[1] (to be referred to as Part 1 hereinafter) of this series, the low-frequency dielectric behavior of nanofiltration (NF) membranes have been studied. In Part 1, we proposed an expression for describing low-frequency relaxation by which the structural and electrical parameters such as the pore radius, thickness of the active layer of the NF membrane, surface charged density and zeta potential on the pore wall were obtained. In short, Part 1 demonstrated that dielectric spectroscopy method has obvious advantage in obtaining information inside separation membranes used in liquid systems. However, some key issues, such as the calculations of volumetric charge density and ion solvation energy barrier, are still unresolved. In fact, it is impossible to obtain these parameters only by analyzing low-frequency relaxation. They are particularly important for discussing ion transport process when the membranes are in working conditions (*i.e.* when membranes were immersed in solution). This is because that they can determine the membrane flux and ion selectivity:[2] the membrane volumetric charge density strongly influence the electrostatic interaction between the membrane and the ions,[3] and the ion solvation energy barrier can represent the degree of dielectric exclusion effect.[4] Analyzing the dielectric relaxation occurring at high frequency can provide information on the electrical properties of the constituent phases of the membrane–electrolyte solution system, especially the membrane and the pore inside the membrane.

Several experimental methods, such as measurement of membrane potential, streaming potential, zeta potential and salt permeability, have been used widely to characterize the NF membrane.[4–8] Some of these methods can obtain information on the pore radius of the membrane from which the membrane volumetric charge density can be calculated. Furthermore, other researches focus on predicting membrane performance through theoretical model with the help of assumed parameters, such as the pore radius and membrane relative permittivity.[9,10] Besides, the researches on checking the applicability of the existing model by comparing theoretical with experimental results, and discussing the influence of dielectric exclusion and Donnan exclusion on ion permeability of membrane have been reported.[11–13] In the former methods, the factors that affect ion transport have not been analyzed, while by the latter methods, it is difficult to give accurate parameters on membrane performance because just assumed parameters were used. Dielectric analysis based on appropriate model can compensate for these defects.

Numerous valuable researches on separation membrane by dielectric spectroscopy or electrical impedance spectroscopy (EIS) have been reported.[14–23] Among them, the works from Coster and co-workers are representative. They determined the stability of supporting liquid membrane,[14] characterized the

College of Chemistry, Beijing Normal University, Beijing 100875, China. E-mail: zhaoks@bnu.edu.cn; Tel: +86-010-58805856

† Electronic supplementary information (ESI) available. See DOI: 10.1039/c4ra13598a

electrical properties and porosity of ultrafiltration membranes,[13] discussed fouling of reverse osmosis membranes,[16] and investigated the electrical properties of BSA-fouling of ion exchange membrane by EIS.[17] Besides, Benavente *et al.* studied the influence of polysulfone membranes that modified with polyethylene glycol and lignosulfate on the electrical properties of membrane.[18] In our previous studies,[24] an effective method to calculate the inner parameters of multi-membrane under solution was proposed, and have been adapted to detect the structural and electrical properties of NF membrane.[25–27]

In fact, the dielectric analysis method has been widely used to study various heterogeneous systems to obtain inner information of constituent phases of these systems.[28] For the membrane–solution systems, the relative permittivity and conductivity of the membrane phase and solution phase, ε_m,ε_w,κ_m,κ_w, can be calculated. Among these phase parameters, the relative permittivity of the membrane ε_m is very significant because it is essential to calculate the ion solvation energy barrier that characterize the selectivity of membrane. In addition, by these phase parameters, the porosity of membrane and membrane volumetric charge density can be evaluated. Moreover, taking the advantages of the dielectric analysis method, namely *in situ* and non-invasive measurement to the system,[29,30] all the parameters coupled with the transport models can describe the behavior of membrane in real separation process, which is undoubtedly effective for discussing ions permeability.

In the present paper, the dielectric measurements for three types of nanofiltration membrane (NF90, NF-, NF270) immersed in different electrolyte solutions were carried out over a frequency range from 40 Hz to 110 MHz. Choosing these membranes is because that the structural and electrical parameters of these membranes, especially their pore radius and volumetric charge density are different from one another. The objective of this paper is to explain the high-frequency relaxation behavior and obtain the parameters of membrane and electrolyte solution phase, especially the relative permittivity of the NF membrane in varying electrolyte solutions. The relative permittivity is an indispensable value for calculating more electrical parameters by which we estimate the ion permeability and selectivity of the membrane, the porosity of the membrane and membrane volumetric charge density by combining with TMS transport model. We will also derive the expressions describing the relation between the concentration of co- and counter-ions in membrane pores and membrane volumetric charge density. The ion permeability in three types of membranes respectively will also be suggested by using the ion solvation energy barrier.

2. Theory and method

2.1 Dielectric analysis

The dielectric analysis in this work refers to the calculation of electric parameters of membrane phase and electrolyte solution phase by using the dielectric parameters observed in dielectric spectra. From these phase parameters, the porosity of membrane, membrane volumetric charge density, and ion solvation energy barrier can be calculated. Therefore, getting the phase parameters is crucial in this work. For a heterogeneous system comprised of nearly insulated polymer membrane and weak conductivity solutions, an interface exists between membrane and solution. According to Maxwell–Wagner interface polarization theory,[31] when an AC electric field is applied to the solution–membrane–solution system, the charges will accumulate on the interface and an inductive field produce to keep the continuity of the electric current. Under such conditions, the relative permittivity and conductivity of membrane phase and solution phase (ε_m, κ_m and ε_w, κ_w) meet following relation: $\varepsilon_m/\kappa_m \neq \varepsilon_w/\kappa_w$ (subscript m and w denote the membrane phase and solution phase, respectively), leading to interface polarization, and a relaxation can be observed by measuring frequency dependence of the complex permittivity of the whole system.

In this work, the membrane is sandwiched between two solution phase, so the measuring system can be considered as a solution–membrane–solution construction.[28,29] From dielectric point of view, when the solutions at both sides of the membrane are the same, the system can be represented to be a series combination of a membrane phase with a complex capacitance C_m^* and a solution phase with a complex capacitance C_w^*. The equivalent circuit of the system is shown in Fig. 1(a), each phase consists of a resistor (of conductance G) in parallel with a capacitor (of capacitance C). It should be noted that what observed experimentally is the frequency dependence of apparent capacitance $C(f)$ and apparent conductance $G(f)$ of the whole system represented by equivalent circuit Fig. 1(b).

Based on the MW theory, the complex capacitance C^* of the whole measuring system is represented by eqn (1),

$$\frac{1}{C^*} = \frac{1}{C_m^*} + \frac{1}{C_w^*} \tag{1}$$

where the complex capacitance can be defined as

$$C^* \equiv \frac{G^*}{j\omega} = C + \frac{G}{j\omega} \tag{2}$$

Eqn (2) can also be written by the complex relative permittivity

$$\varepsilon^* = \varepsilon' - j\varepsilon'' = \varepsilon + \frac{\kappa}{j\omega\varepsilon_0} \tag{3}$$

where ε' and ε'' are real and imaginary part of the complex permittivity, ε and κ are the relative permittivity and the conductivity of the system, respectively, ω ($=2\pi f$) is angular

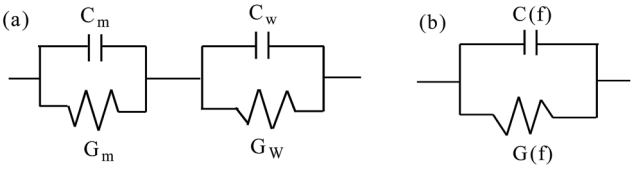

Fig. 1 (a) A circuit model to simulate a bilamellar structure composed of nanofiltration membrane and an electrolyte solution; (b) equivalent capacitance $C(f)$ and conductance $G(f)$ for the whole cell system.

frequency, ε_0 (=8.8541 × 10^{-12} F m^{-1}) is the vacuum permittivity, and j is the imaginary unit.

By substituting the eqn (2) into (1), the capacitance and conductance can be expressed by that of the constituent phases. Hanai *et al.* derived a series of expressions about the relations between phase parameters *i.e.* the capacitance and conductance of membrane and solution phase C_m,C_w,G_m,G_w (see Fig. 1(a)) and dielectric parameters (*i.e.* the limiting values of C and G at high (subscript h) and low (subscript l) frequencies C_l,C_h,G_l,G_h).[32] According to these equations, the values of C_m,C_w,G_m,G_w (or ε_m,κ_m,ε_w,κ_w) can be calculated. The corresponding calculation formulas and computational procedures are listed in ESI.† For additional information about expressions, refer to literature.[27]

2.2 Transport models of charged membrane—TMS model

NF membrane is often characterized by three adjustable parameters, pore radius, volumetric charge density, and effective membrane thickness. The three parameters, especially the membrane volumetric charge density play an important role in the understanding of separation mechanism and ion permeability. Theoretically, combining the results of dielectric analysis with transport model, the value of volumetric charge density can be obtained. In this work, we choose the Donnan exclusion—TMS model.

In TMS model, the membrane is described as a gel-phase, ion concentration and electric potential distributed uniformly in the membrane. The basic equations of the model consist of Donnan equation describing the ion dispersions in membrane and in bulk solution and the Nernst–Planck equation that is related to the ion transport in membrane. Besides, the electroneutrality conditions in membrane and solution two phases defined below must be taken into account when the ion partitioning coefficients is calculated. The important parameter of above equations, ion partitioning coefficients, is given by

$$k_i = \frac{c_i^m}{c_i} = \exp\left(-\frac{z_i F \Delta\phi}{RT}\right) \tag{4}$$

where c_i^m and c_i are the concentration (mol m^{-3}) of ion i in membrane and in electrolyte solutions respectively, z_i is the valence of ion i; $\Delta\phi$ is Donnan potential difference (V), F is Faraday constant, T is absolute temperature. Combining eqn (4) with the electroneutrality conditions inside membrane and external solutions respectively (see eqn (5) and (6)), the expression of counter- and co-ions concentration in membrane by considering Donnan exclusion can be obtained (see eqn (7)–(11))

$$z_1 c_1^m + z_2 c_2^m + c_e = 0 \tag{5}$$

$$z_1 c_1^w + z_2 c_2^w = 0 \tag{6}$$

where subscript 1 and 2 denote the counter- and co-ion, respectively, c_e represents the concentration of the fixed charge in membrane.

For 1 : 1 and 2 : 1 type-electrolyte solution, the concentration of co- and counter-ions in membrane can be expressed as:

$$c_1^m = \frac{|c_e| + \sqrt{(|c_e|)^2 + 4(c_1^w)^2}}{2} \tag{7a}$$

$$c_2^m = \frac{-|c_e| + \sqrt{(|c_e|)^2 + 4(c_1^w)^2}}{2} \tag{7b}$$

and

$$c_1^m = \left(|c_e|^3/27 + (c_1^w)^3/2 + \sqrt{|c_e|^3(c_1^w)^3/27 + (c_1^w)^6/4}\right)^{1/3} + \left(|c_e|^3/27 + (c_1^w)^3/2 - \sqrt{|c_e|^3(c_1^w)^3/27 + (c_1^w)^6/4}\right)^{1/3} + |c_e|/3 \tag{8a}$$

$$c_2^m = \left(\left(|c_e|^3/27 + (c_1^w)^3/2 + \sqrt{|c_e|^3(c_1^w)^3/27 + (c_1^w)^6/4}\right)^{1/3} + \left(|c_e|^3/27 + (c_1^w)^3/2 - \sqrt{|c_e|^3(c_1^w)^3/27 + (c_1^w)^6/4}\right)^{1/3}\right) \times /2 - |c_e|/3 \tag{8b}$$

For 1 : 2 type-electrolyte solution, the concentration of co- and counter-ions in membrane can be expressed as:

When $144(c_1^w)^6 - 4|c_e|^3(c_1^w)^3 > 0$

$$c_1^m = \left(\left(-|c_e|^3/27 + 4(c_1^w)^3 + \sqrt{16(c_1^w)^6 - 4|c_e|^3(c_1^w)^3/9}\right)^{1/3} + \left(-|c_e|^3/27 + 4(c_1^w)^3 - \sqrt{16(c_1^w)^6 - 4|c_e|^3(c_1^w)^3/9}\right)^{1/3}\right) \times /2 + |c_e|/3 \tag{9a}$$

$$c_2^m = \left(-|c_e|^3/27 + 4(c_1^w)^3 + \sqrt{16(c_1^w)^6 - 4|c_e|^3(c_1^w)^3/9}\right)^{1/3} + \left(-|c_e|^3/27 + 4(c_1^w)^3 - \sqrt{16(c_1^w)^6 - 4|c_e|^3(c_1^w)^3/9}\right)^{1/3} - |c_e|/3 \tag{9b}$$

When $144(c_1^w)^6 - 4|c_e|^3(c_1^w)^3 < 0$

$$c_1^m = |c_e|/3\cos(\arccos(108(c_1^w)^3/|c_e|^3 - 1)/3) + |c_e|/3 \tag{10a}$$

$$c_2^m = 2|c_e|/3\cos(\arccos(108(c_1^w)^3/|c_e|^3 - 1)/3) - |c_e|/3 \tag{10b}$$

For 2 : 2 type-electrolyte solution, the corresponding concentrations are expressed as:

$$c_1^{\mathrm{m}} = \frac{|c_e| + \sqrt{(|c_e|)^2 + 16(c_1^{\mathrm{w}})^2}}{4} \quad (11a)$$

$$c_2^{\mathrm{m}} = \frac{|c_e| + \sqrt{(|c_e|)^2 + 16(c_1^{\mathrm{w}})^2}}{4} - \frac{|c_e|}{2} \quad (11b)$$

Combining these concentration expressions deduced with the conductivities (κ_m and κ_w) of membrane and electrolyte solution which are obtained through dielectric analysis, membrane volumetric charge density c_e can be estimated. Substituting c_e back into eqn (7)–(11), the values of these concentration that considered Donnan exclusion can be calculated. These parameters will provide essential support for discussing the influence factors on ion permeability of membrane.

3. Experimental

3.1 Nanofiltration membranes

The NF membranes measured and analyzed in this study are exactly the same as that used in our previous work,[1] *i.e.* NF90, NF- and NF270. They are made of three different layers: a thick and large mesoporous polysulfone support layer, a thin polyamide active layer and an intermediate polysulfone layer. The thin active layer and the intermediate layer, commonly known as effective layer, was measured as a standalone membrane although only the thin active layer play a key role in the separation process, because it is impossible that the very thin active layer was peeled off from the NF membrane. The membranes may be negatively charged in solution by partial dissociation of the carboxyl groups (–COOH). Thus, counter-ions are cations in the electrolyte solutions, while co-ions are anions in the electrolyte solutions. The support layer of the membranes was peeled off, and the remaining part of the membrane includes the active layer and the intermediate layer as mentioned above, its thickness is about 0.2 μm, measured with a micrometer.

3.2 Dielectric measurements

Dielectric measurements of the three membranes in varying electrolyte concentrations were carried out with HP4294A Precision Impedance Analyzer. The measuring cell system and the measuring condition are the same as described in our previous work[1] and the literatures.[29,34] The membrane (hereinafter, the term membrane refer to the effective layer of NF membrane)/electrolyte solution systems were measured in the same way and conditions described in Part 1.[1]

In this paper, we take NF90 membranes–K_2SO_4 solution as an example to illustrate the dielectric analysis processes. But, the analysis results for all three membranes (NF90, NF- and NF270 membrane) are discussed. All the raw data were subjected to certain corrections for the errors arising from residual inductance due to the cell assembly,[35] and the detail is also described in the Part 1.[1] The relative permittivity ε and conductivity κ were determined by following equations $\varepsilon = C_s/C_l$ and $\kappa = G_s\varepsilon_0/C_l$ (ε_0 is the permittivity of vacuum).

4. Result and discussion

4.1 Dielectric analysis of the NF membrane–electrolyte solutions system

4.1.1 Dielectric spectroscopy. Fig. 2 shows three-dimensional representations for the concentration dependence of dielectric spectra of the system of NF90 membrane in K_2SO_4 solution in the concentration range of 0.05–7 mol m^{-3}, which is similar to the dielectric spectra of NF90 membrane in $MgCl_2$ solution shown in Part 1,[1] two relaxations can be observed (other systems measured in this work showed similar dielectric spectra). The low-frequency relaxation around at 10^2 Hz caused by the counterion polarization in the membrane pores had been discussed thoroughly in Part 1.[1] This paper focuses solely on the analysis and discussion of high-frequency relaxation. From Fig. 2, it is obvious that it showed a large relaxation intensity and its characteristic frequency shifts to higher frequency as electrolyte concentration increases as illustrated by the arrows.

4.1.2 Estimation of dielectric parameters and determination of relaxation mechanism. In order to obtain the electric properties of the constituent phases of the membrane–solution system (*i.e.* the phase parameters of the system) and the inner information of the membrane in electrolyte solution, it is necessary to estimate the value of dielectric parameters mentioned in Section 2.1. For clarity, we took the system with NF90 membrane in 0.05 mol m^{-3} K_2SO_4 solution as an example (see Fig. 3, it is the two-dimensional representation of Fig. 2 when the concentration of K_2SO_4 is 0.05 mol m^{-3}) to introduce how these parameters were determined from the dielectric spectrum.

Fig. 3(a) and (b) show the frequency dependence of the relative permittivity and the conductivity in different electrolyte concentrations for the NF90 membrane–K_2SO_4 system, respectively. In Fig. 3, ε_l,ε_h,κ_l,κ_h termed dielectric parameters in this paper, indicate the limiting value of relative permittivity and conductivity at low and high frequencies, respectively, and f_0 is characteristic relaxation frequency. Generally, in order to estimate dielectric parameters, the "model function method" in which Cole–Cole empirical equation is used to fit dielectric data is often employed.[35] However, when the relaxation profile is utterly clear, so called "model free method" are also adopted, *i.e.* determine the dielectric parameters by plotting. Fig. 4(a) and (b) show the complex plane plots of relative permittivity and conductivity, respectively, and Fig. 4(c) shows the frequency dependence of dielectric loss. The values of ε'' and κ'' were calculated according to following relations respectively, the values of ε_l,ε_h,κ_l,κ_h, and f_0 were determined from these figures:

$$\varepsilon'' = \frac{\kappa - \kappa_l}{\omega\varepsilon_0} \quad (12)$$

$$\kappa'' = \omega\varepsilon_0(\varepsilon - \varepsilon_h) \quad (13)$$

To examine if the dielectric parameters obtained above were accurate, we fitted the dielectric spectrum data using Cole–Cole

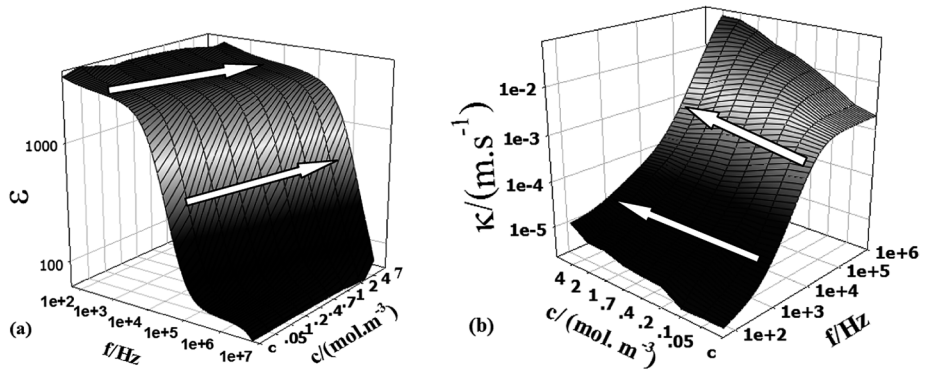

Fig. 2 Frequency dependence of the relative permittivity ε (a) and conductivity κ (b) for the system composed of the NF90 membrane and the compartments filled with K_2SO_4 aqueous solution of various concentrations.

equation in trigonometric function (eqn (14)), and only ε_l,ε_h and f_0 were obtained, κ_l and κ_h were obtained according to the method described in Section 3.2.1 of Part 1.[1]

$$\varepsilon(f) = \varepsilon_h + \frac{(\varepsilon_l - \varepsilon_h)\left[1 + \left(\frac{f}{f_0}\right)^{\beta}\cos\left(\frac{\pi}{2}\beta\right)\right]}{1 + 2\left(\frac{f}{f_0}\right)^{\beta}\cos\left(\frac{\pi}{2}\beta\right) + \left(\frac{f}{f_0}\right)^{2\beta}} \quad (14)$$

where f is the measured frequency, and β is the distribution coefficient of relaxation time ($0 < \beta \leq 1$), which reflects the complexity of inner structure of the system.[25] The values of dielectric parameters obtained by fitting dielectric spectra are almost the same as that by model free method. The dielectric parameters for other systems were also obtained in the same way and are summarized in Table 1.

It is obvious from Table 1 that the dielectric increment $\Delta\varepsilon$ ($=\varepsilon_l - \varepsilon_h$) is almost invariable as concentration increases, whereas the characteristic frequency f_0 and conductivity increment $\Delta\kappa$ ($=\kappa_h - \kappa_l$) depend linearly on the concentration, as shown in Fig. 5. According to our previous researches on membrane–solution system[28–30,32,34] and the literatures,[33,36] this result indicates a distinctive feature of the interfacial polarization. Therefore, we believe that the high frequency relaxation is caused by the interfacial polarization occurring at the interface between whole membrane and solution, and the analysis method elaborated in Section 2.1 is suitable for analyzing this high-frequency relaxation.

4.1.3 Calculation of phase parameters and comments on the results. In order to explore the structural and electrical properties of the membrane under varying electrolyte solutions, it is indispensable step to calculate the phase parameters. By using the method described in Section 2.1 the phase parameters (ε_m,κ_m,ε_w,κ_w) for all of NF90 membrane–electrolyte solution systems were calculated from the dielectric parameters in Table 1, and the results are listed in Table 2.

Relative permittivity and conductivity of the electrolyte solution ε_w and κ_w. It can be seen from Table 2 that the relative permittivity of electrolyte solutions ε_w is nearly invariable with the electrolyte concentration, and its average value is about 80.37. This is a reasonable value comparing with that of pure water (about 80 at 21–22 °C).[37] Furthermore, the reliability of this result was enhanced by a independent measurement: the dielectric measurements of K_2SO_4 solutions with various concentrations were carried out under the same conditions with the membrane–solution systems, and the relative permittivity and conductivity ε'_w, κ'_w without membrane at various concentrations were obtained (also listed in Table 2). The values of ε'_w show surprisingly closely with ε_w obtained by dielectric analysis. By comparing ε_w and κ_w with ε'_w and κ'_w, we find that the values of $\varepsilon_w/\varepsilon'_w$ and κ_w/κ'_w are all close to 1 and independent of the electrolyte concentration (see Table 2). This means that ε_w and κ_w of K_2SO_4 solution obtained by analyzing dielectric spectrum

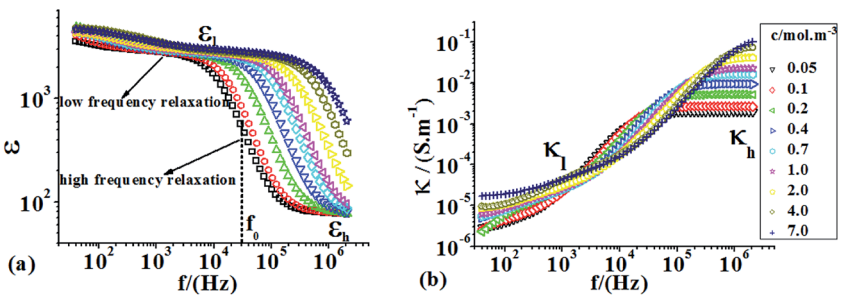

Fig. 3 Frequency dependences of (a) relative permittivity ε and (b) conductivity κ for the cell systems with NF90 membrane in K_2SO_4 aqueous solutions.

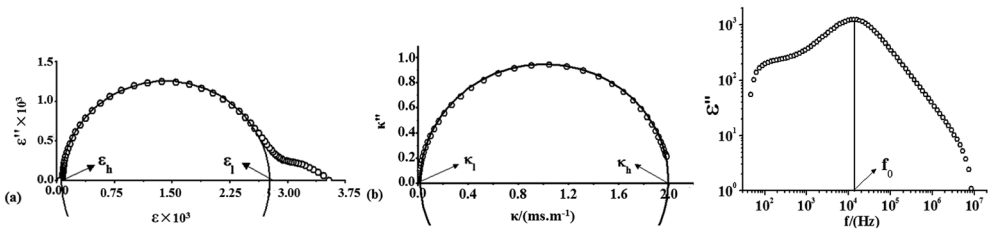

Fig. 4 Frequency dependence of (a) relative permittivity ε and (b) conductivity κ for the cell systems with NF90 membrane in 0.05 mol m^{-3} K_2SO_4 aqueous solution.

are in good agreement with their actual value, showing that strict dielectric analysis can give accurate inner information of the membrane. The values of $\varepsilon_w/\varepsilon_w'$ and κ_w/κ_w' for other seven electrolyte solutions (NaCl, KCl, $MgCl_2$, $CuCl_2$, Na_2SO_4, $MgSO_4$, $CuSO_4$) are similar to that of K_2SO_4. ε_w will play an important role to evaluate permeability of pore and ion solvation energy barrier.

Relative permittivity and conductivity of the membrane ε_m and κ_m. It is worth mentioning that the relative permittivity of membrane ε_m obtained in this work is vital to calculate accurately the porosity of membrane and ion solvation energy barrier because it is the permittivity of wet membrane rather than that of dry membrane. It is clear from Table 2 that the value of ε_m is almost independent of the electrolyte concentration (actually, ε_m is also independent of the kind of electrolyte solutions, as can be seen in Table 3 below), and the average value of ε_m, 2.266, is larger than that of the polymer matrix of the membrane in dry state (relative permittivity of polyamide is about 1.68). For NF- and NF270 membrane, their ε_m are all larger than that in dry state as well as shown in Table 3 (the relative permittivity of mixed aromatic amines and heterocyclic aliphatic amines, which are main components of NF- and NF270, are about 3–4). This is easy to understand because of the permeation of water with high relative permittivity into the porous membrane of low relative permittivity. In this case, ε_m is simply expressed by eqn (15). Here, it should be noted that the value of ε_w is regarded as 80, this is a rough approximation. This is because that the membrane contains two parts: a very thin active layer and a relative porous intermediate layer, the water in the membrane mainly comes from the porous intermediate layer.

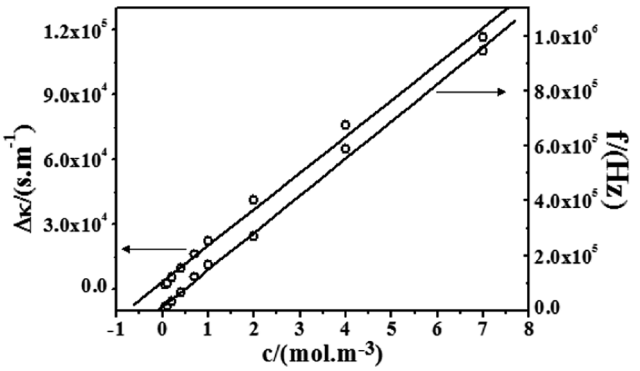

Fig. 5 Relaxation increment of relative permittivity $\Delta\kappa$ and the character frequency f_0 of high-frequency relaxation for the NF90 membrane in K_2SO_4 electrolyte solutions against electrolyte concentration c.

$$\varepsilon_m = \varepsilon_w f_w + \varepsilon_m'(1 - f_w) \quad (15)$$

where f_w and $1 - f_w$ are the volume fraction of water in the whole membrane phase and in membrane matrix of the membrane phase, ε_m' is the relative permittivity of dry polymers. It should be noted here that ε_m in eqn (15) is obtained from dielectric analysis, and it is a mixed value including the contributions of membrane matrix and the water in the pores of membrane.

Taking the relative permittivity of dry NF90 membrane as 1.68 and substituting ε_m and ε_w listed in Table 2 into eqn (15), the values of f_w at various concentrations of K_2SO_4 were calculated. The results showed that f_w decreases sharply with the increase of electrolyte concentration within lower concentration and finally tends to remain unchanged as shown in Fig. 6(a),

Table 1 Dielectric parameters obtained by fitting with eqn (16) for NF90 membrane in K_2SO_4

c (mol m^{-3})	ε_l	ε_h	$\Delta\varepsilon$	κ_l (μS m^{-1})	κ_h (mS m^{-1})	$\Delta\kappa$ (μS m^{-1})	f_0 (Hz)
0.05	2559.11	79.78	2479.33	12.46	2.002	1989.54	11 531
0.1	2558.34	79.85	2478.49	16.78	2.725	2708.22	18 486
0.2	2555.32	78.80	2476.52	17.36	5.299	5281.64	34 687
0.4	2553.95	79.06	2474.89	23.20	9.584	9560.8	65 086
0.7	2558.02	78.81	2479.21	38.58	16.13	16091.42	122 125
1.0	2555.46	78.75	2476.71	50.56	22.45	22399.44	167 287
2.0	2552.33	78.87	2473.46	90.37	41.45	41359.63	268 193
4.0	2557.42	78.80	2478.62	172.0	76.22	76 048	588 965
7.0	2550.99	78.74	2472.25	270.9	117.0	116729.1	944 223

Table 2 Phase parameters calculated for the systems of NF90 membrane and K_2SO_4 solutions

c (mol m^{-3})	ε_m	ε_w	κ_m (nS m^{-1})	κ_w (mS m^{-1})	ε_w'	κ_w' (mS m^{-1})
0.05	2.741	80.25	19.23	2.074	80.12	2.045
0.1	2.323	80.61	13.44	2.846	80.33	2.829
0.2	2.401	80.53	14.75	5.528	80.69	5.152
0.4	2.313	80.14	20.49	10.01	80.27	10.00
0.7	2.082	80.40	30.90	16.96	80.66	17.28
1.0	2.115	80.36	42.39	23.59	80.82	24.58
2.0	2.086	80.04	76.35	43.04	80.29	44.39
4.0	2.045	80.44	142.2	80.38	80.47	83.39
7.0	1.995	80.56	218.2	123.4	80.73	134.6

Table 3 The mean value of ε_m at various electrolyte concentrations for all the measured systems

	Membrane		
Electrolytes	NF90	NF-	NF270
NaCl	2.729	3.408	3.741
KCl	2.912	3.966	4.228
$MgCl_2$	2.187	3.552	7.532
$CuCl_2$	2.145	3.981	6.774
Na_2SO_4	2.201	6.021	8.924
K_2SO_4	2.065	3.292	3.839
$MgSO_4$	2.312	6.315	5.419
$CuSO_4$	2.207	5.542	7.919
Average	2.395	4.510	6.047

when concentration of K_2SO_4 is above 0.7 mol m^{-3} f_w is about 0.004, indicating that the water content in membrane is very low. Therefore, we can speculate that the membrane has a compact structure and ions are hard to pass through the membrane, leading that ions can be effectively retained in the membrane.

The concentration dependency of ε_m has similar changing trend with that of f_w (Fig. 6(b)), *i.e.* both of ε_m and f_w decrease sharply near the concentration of 0.7 mol m^{-3}. The reason may be interpreted as follow: because the membrane is electrical charged, when the counter-ions enter the membrane pores, electrostatic repulsion between polymeric backbones will be shielded gradually, giving rise to aggregate and reunite between polymer chains in a relatively compact state. Accompanied with this change, f_w decreased, so did the relative permittivity of the membrane ε_m. While when fixed charges were shielded completely because of the ions permeating into the membrane, increasing the concentration of electrolyte solution will no longer impact on the aggregation state of polymer backbones. As a result, f_w and ε_m have no change over the concentration range of 1–7 mol m^{-3}. Therefore, in following calculations, we took the mean value of ε_m (2.065 for NF90 membrane in K_2SO_4) in varying electrolyte concentrations as the relative permittivity of membrane. The mean values for three kinds of membranes NF90, NF- and NF270 in eight electrolyte solutions are listed in Table 3.

From the Table 3 it is obvious that for NF90 membrane ε_m is almost independent of the kind of the electrolyte and has an average of 2.4, while the values for both NF and NF270 membranes are indeterminate for different electrolyte type. ε_m fluctuates between 3.3 and 6.3 and average is about 4.5 for NF-membrane, and it changes ranging from 3.7 to 8.9 and average is about 6.0 for NF270 membrane. These fluctuations of data can be believed to be caused by the error during calculation process because the results in Table 3 are obtained through two times calculation processes starting from raw data. In addition, the values of ε_m for both NF and NF270 membranes are greater than that of NF90. This may be related to the porosity of these membranes.

In our previous paper,[1] we have calculated thickness and pore diameter of the three membranes. The average values of the thickness in different concentrations are 0.2335 μm, 0.2337 μm and 0.2334 μm, and the average values of pore diameter are 0.2838, 0.3250, 0.3582 nm for NF90, NF- and NF270 membrane, respectively. Obviously, the pore diameter for NF- and NF270 membrane are approximately equal but greater than that of NF90. Therefore, the reason of the difference in relative permittivity between three membranes can be explained as follows: the membrane with high water content has higher relative permittivity, therefore the values of ε_m for both NF- and NF270 membrane are greater than that of NF90. This can also be supported by the data of porosity of the three membranes (see a later Table 5).

To investigate the selectivity and permeability of ions in the NF membranes, the dependency of membrane conductivity κ_m on electrolyte concentration for the three membranes in eight

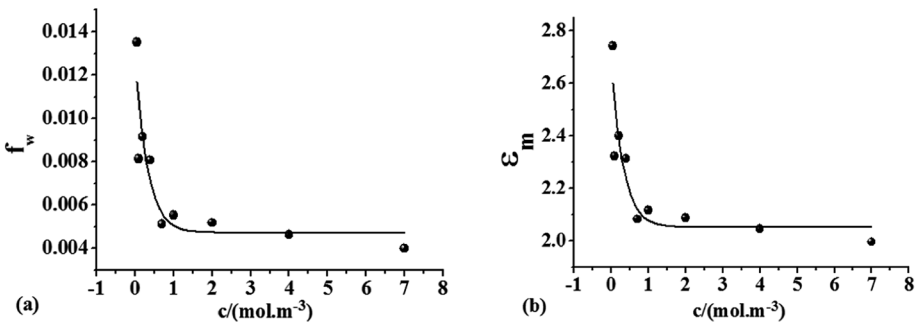

Fig. 6 Concentration dependence of f_w (a) and ε_m (b) for system of NF90 membrane in K_2SO_4 electrolyte solutions.

electrolyte solutions was plotted in Fig. 7. It is obvious that κ_m increases linearly with increasing electrolyte concentration for each system, however, the increase rates are different each other. For different types of electrolyte solutions, the increase rate of κ_m for NF- membranes in four types of electrolyte solutions follow the trend: 1 : 2 > 1 : 1 > 2 : 1 > 2 : 2. This is because that under AC field, ions transporting into membrane was influenced by dielectric exclusion, Donnan exclusion and steric hindrance, because the interaction between the ions with different valences and three kinds of membranes respectively are not the same, such, the degree of difficulty that the ions of different types of electrolyte transfer into membrane are also different. As a result, there are differences in κ_m for different types of electrolyte.

For NF-membrane, univalent counter-ions are easier to transport into the membrane than bivalent counter-ions. The lower the valence of co-ions, the easier the electrolyte transporting into the membrane. It can be seen from Fig. 7 that, for different types of electrolytes, the increase rate of κ_m for NF90 membrane in four electrolyte solutions follow the trend: 1 : 1 > 2 : 1 > 1 : 2 > 2 : 2, while for NF270, it seems irregularly. In short, increasing rate of κ_m for the three types of NF membranes in different types of electrolytes are various, showing that the interaction between ions and membrane matrix are different, this is because these membranes have different structural and electrical properties, *i.e.* pore radius, membrane volumetric charge density and porosity of the membrane. Therefore, the difficulty for electrolytes transporting into the three types of NF membranes are different. We will further discuss the influence factors of ions transport by combining the TMS model and the ion solvation energy barrier.

4.2 Calculation of some important parameters of membrane

4.2.1 Porosity of membrane. According to the discussions in Section 4.1.3, the relative permittivity ε_m or capacitance C_m of the membrane is from the contributions of two parts: polymer matrix and solution in membrane pores,[14] as expressed by following equation:

$$C_m = C'_m + C_p = [\varepsilon_p\varepsilon_0 Sp]/a + [\varepsilon'_m\varepsilon_0(1-p)S]/a \quad (16)$$

where C'_m is capacitance of the polymer matrix. C_p and ε_p are the capacitance and relative permittivity of the pore filled with electrolyte solution; p and a are porosity and thickness of the membrane, respectively. The meaning of other symbols in eqn (16) are the same to that defined in earlier sections.

From eqn (16), p can be represented as

$$p = [(aC_m/\varepsilon_0 A) - \varepsilon'_m]/[\varepsilon_p - \varepsilon'_m] \quad (17)$$

In this formula, the relative permittivity of dry polymers ε'_m is known (see Section 4.1.3), so C_m can be calculated according to $\varepsilon_m = C_m(a/S\varepsilon_0)$, where the membrane thickness a for three membrane have been obtained in Part 1.[1] While ε_p was calculated by following equation:[38]

$$\varepsilon_p = \varepsilon_w - 2(\varepsilon_w - \varepsilon_d)\left(\frac{d}{b}\right) + (\varepsilon_w - \varepsilon_d)\left(\frac{d}{b}\right)^2 \quad (18)$$

Eqn (18) shows that the pore is consisted of one layer of oriented water molecules at the pore-wall (the relative permittivity and the thickness of the water layer are ε_d and d respectively) and solution inside the pore which is different from bulk solution because under AC field the rotation of the water molecules in the pore is restrained. So, relative permittivity ε_p inside the pore is different from that ε_w of bulk water. According to literature,[38] the values of ε_d and d are 6 and 0.28 nm respectively. The pore radius have also been obtained in Part 1. The calculated ε_p are listed in Table 4.

By substituting ε_p in Table 4 into eqn (17), the porosity of three NF membranes p in different electrolyte solutions were calculated and are listed in Table 5. It is clear that for any type of membrane, the porosity in different electrolytes has no significant differences, and the porosity has a sequence of NF270 > NF- > NF90. For the convenience of comparison, the dependency of membrane conductivity κ_m of three membranes on K_2SO_4 concentration c were plotted in Fig. 8, it is obvious that the increase rate of κ_m of three membranes as K_2SO_4 concentration c are different: NF270 > NF- > NF90, this sequence is in

Table 4 Pore dielectric constant ε_p of NF membranes in different solutions calculated using eqn (20)

Electrolyte	NaCl	KCl	$MgCl_2$	$CuCl_2$	Na_2SO_4	K_2SO_4	$MgSO_4$	$CuSO_4$
NF90	31.0	31.0	31.0	31.0	31.0	31.0	31.0	31.0
NF-	31.8	31.8	31.5	31.9	31.9	31.8	31.8	31.9
NF270	32.9	32.8	32.9	33.5	33.4	33.7	33.7	33.8

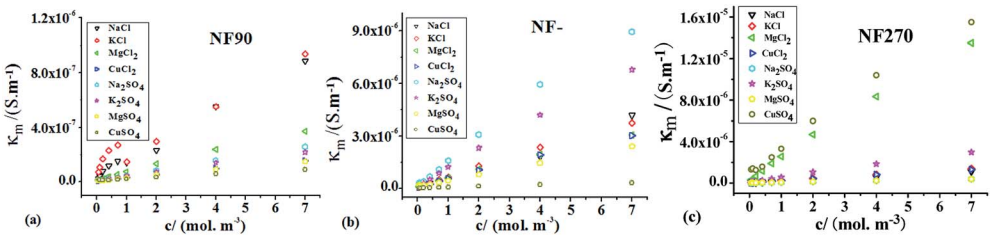

Fig. 7 Dependence of conductivity of membrane κ_m on solution concentration c for systems composed of NF membranes and eight kinds of electrolytes: (a) NF90; (b) NF-; (c) NF270.

Table 5 Porosity of NF membranes for all the measured systems

Electrolyte solutions	$p_{(NF90)}$ (%)	$p_{(NF-)}$ (%)	$p_{(NF270)}$ (%)
NaCl	3.24	5.33	6.15
KCl	3.85	7.12	7.69
$MgCl_2$	1.73	6.20	18.7
$CuCl_2$	1.59	7.60	16.0
Na_2SO_4	1.78	14.3	22.7
K_2SO_4	2.00	5.34	6.73
$MgSO_4$	2.84	15.4	11.7
$CuSO_4$	1.80	12.7	19.4
Average	2.35	9.25	13.6

line with the porosity of the three membranes. Because the magnitude of κ_m is proportional to the amount of electrolyte in membrane as discussed above, the difference in κ_m between the three membranes suggested the possibility that the magnitude of the porosity influences ions transporting into membrane.

4.2.2 Calculation of concentrations of co- and counter-ions in membrane pore. Returning to Table 2, the conductivity of membrane and solution phase, κ_m and κ_w, increase with the increment of electrolyte concentration c, and the value of κ_m is much smaller than that of κ_w because κ_m is a mixed value including the contribution of the polymer. It is should be mentioned that maybe the value of κ_m is greater than that of κ_w for the case of inorganic membrane in electrolyte solution, such as porous alumina membrane.[39] κ_m/κ_w, was plotted as a function of c in Fig. 9. It is obvious that κ_m/κ_w is far less than 1, and decreases sharply at low concentrations and then reaches a stable value when the concentration is above 0.5 mol m^{-3}, showing a typical phenomenon of ions through charged membrane as described by Donnan exclusion.[31,40] Therefore, the membrane volumetric charge density can be estimated according to the variation of the conductivity in membrane and solution phase.

In our previous work,[28] a certain relation among κ_m/κ_w, the ion concentrations in membrane and in solution, and transport numbers of ion in bulk solution had been derived as the following.

$$\frac{\kappa_m}{\kappa_w} = \frac{U_1^m}{U_1^w}\frac{c_1^m t_1^w + c_2^m t_2^w}{c_1^w t_1^w + c_2^w t_2^w} \quad (19)$$

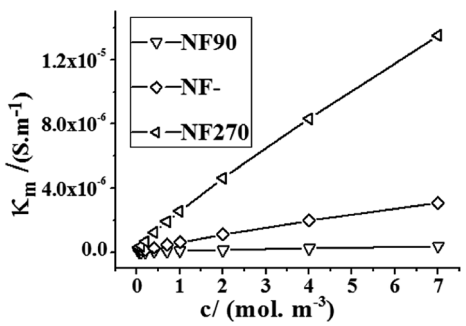

Fig. 8 Concentration dependence of κ_m of NF90, NF- and NF270 in K_2SO_4 electrolyte solutions.

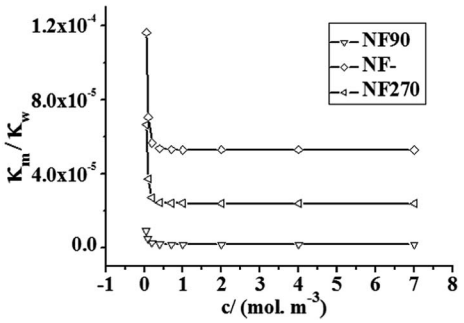

Fig. 9 Concentration dependence of κ_m/κ_w of NF90, NF- and NF270 in K_2SO_4 electrolyte solutions.

where subscript 1 and 2 represent counter-ion and co-ion, U_i^m and U_i^w are the mobility of ions in membrane and solution respectively, c_i^m and c_i^w are the concentration of ions in membrane and solution respectively, t_1^w and t_2^w are the transport numbers of counter-ion and co-ion in solution, respectively. Because the experiment results show that the distribution of ions in solution and in membrane obeys Donnan equilibrium principle, we adopted the TMS model in this study. Combining TMS model with eqn (21), the membrane volumetric charge density c_e for all systems were calculated using the phase parameters obtained from dielectric analysis.

Further, by substituting the expressions eqn (7)–(11) into (19), the expression of κ_m/κ_w for 1 : 1, 1 : 2, 2 : 1, and 2 : 2 type-electrolyte solution with two variables were derived. The two variables, U^m and U^w, are defined as $P_1 = U_1^m/U_1^w = U_2^m/U_2^w$, *i.e.*, the ratio of ion mobility in membrane and solution, and $P_2 = c_e$ (*i.e.*, the membrane volumetric charge density). Then, by fitting the κ_m/κ_w obtained experimentally for all membrane systems to the expression of κ_m/κ_w by varying values of P_1 and P_2, the values of c_e for NF90, NF-, NF270 membranes in eight kinds of electrolyte solutions were obtained and the results are listed in Table 6. It is obvious from Table 6 that for any NF membrane, c_e is almost independent of the kinds of electrolyte solutions, and c_e of NF90 is larger than that of NF- and NF270.

By substituting c_e in Table 6 back into eqn (7)–(11), the concentrations of co- and counter-ions were calculated. Table 7 shows the results for the systems of the three membranes and K_2SO_4 solution. For clarity, the dependences of co- and counter-ions concentration in membranes on the electrolyte concentration c for the three NF membrane systems are plotted in Fig. 10. The concentrations of both co-ions c_2^m and counter-ions c_1^m in membrane pore increase linearly as c increased. The only difference between them is their growth rate with c. Specifically, for 1 : 1 and 2 : 2 type-electrolyte solutions in Fig. 10(a), (b), (g) and (h), c_1^m is larger than c_2^m over the whole concentration range, and the growth rate of c_1^m and c_2^m are the same. For 1 : 2 type-electrolyte in Fig. 10(c) and (d), c_1^m is larger than c_2^m while c is relatively low. However, as the growth rate of c_2^m is over than that of c_1^m, c_2^m becomes larger than c_1^m gradually, which can be explained as follows: when c exceeds c_e, the fixed charge in membrane was neutralized gradually, Donnan exclusion was weakened. On the other hand, the concentration of co-ions c_2 is

Table 6 Membrane volumetric charge density c_e of NF membranes for all the measured systems calculated from eqn (7)–(11) and (15)

Membrane	Electrolyte	NaCl	KCl	$MgCl_2$	$CuCl_2$	Na_2SO_4	K_2SO_4	$MgSO_4$	$CuSO_4$	Average
NF90	(c_e (mol m^{-3}))	0.88	0.85	1.13	1.09	0.90	0.81	1.05	1.03	0.97
NF-	(c_e (mol m^{-3}))	0.62	0.36	0.76	0.41	0.55	0.33	0.70	0.34	0.51
NF270	(c_e (mol m^{-3}))	0.69	0.41	0.57	0.55	0.56	0.42	0.59	0.58	0.55

twice that of counter-ions in bulk solution c_1, therefore, c_2^m becomes larger than c_1^m gradually as c increase. The membrane volumetric charge density c_e was determined from the intersection of the lines of co-ions and counter-ions. For 2 : 1 type-electrolyte in Fig. 10(e) and (f), because c_1 is twice that of co-ions c_2 in bulk solutions, the growth rate of c_1^m is larger than c_2^m.

The parameters above obtained, c_e, c_2^m and c_1^m in four types electrolyte solutions, will be used to discuss the influence of Donnan exclusion on the transport of different electrolyte in three membranes in following 4.3 Section.

4.2.3 Ion solvation energy barrier. As we know, the dielectric exclusion is caused by the interactions of ions with the bound charges that induced by the ions at interface between substances of different relative permittivity. Therefore, due to the difference of relative permittivity between membrane pores and solution, when ions transfer from solution with high relative permittivity (about 80) to membrane pores with low relative permittivity (about 31–34, see Table 4), dielectric exclusion occurs, thereupon ion solvation energy barrier arises (which will clearly increase salt rejection). Born solvation energy barrier represents the effect of dielectric exclusion and its magnitude influences the ions entering into the pores. Therefore, by this value, the permeability of ions for different kinds of electrolytes in membrane can be evaluated.

Considering the change of electrostatic free energy (or relative permittivity) of an ion from bulk to membrane pore, based on Born equation[12] in which only the relative permittivity of whole membrane was considered, an expressions of ion solvation energy barrier ΔW_i for ion i was proposed:[40]

$$\Delta W_i = \frac{z_i^2 e^2}{8\pi\varepsilon_o r_s}\left(\left(\frac{1}{\varepsilon_p}+\frac{0.393}{b/r_s\varepsilon_m}\left(1-\frac{\varepsilon_m}{\varepsilon_p}\right)^2\right)-\frac{1}{\varepsilon_w}\right) \quad (20)$$

Table 7 Concentration of co- and counter-ions in pores of NF membranes for all the measured systems

	NF90/K_2SO_4		NF-/K_2SO_4		NF270/K_2SO_4	
c (mol m^{-3})	c_1^m	c_2^m	c_1^m	c_2^m	c_1^m	c_2^m
0.05	0.8080	0.0008	0.3364	0.0044	0.4258	0.0028
0.1	0.8184	0.0060	0.3823	0.0274	0.4584	0.0190
0.2	0.8877	0.0406	0.5439	0.1082	0.5988	0.0892
0.4	1.1764	0.1850	0.9254	0.2989	0.9674	0.2735
0.7	1.7268	0.4601	1.5182	0.5953	1.5550	0.5674
1.0	2.3081	0.7508	2.1154	0.8939	2.1504	0.8650
2.0	4.2877	1.7406	4.1122	1.8923	4.1451	1.8624
4.0	8.2781	3.7358	8.1107	3.8916	8.1426	3.8611
7.0	14.274	6.7338	14.110	6.8912	14.142	6.8606

where r_s is Stokes radius of ion, the meaning of other symbols is the same as defined above. The value of r_s for the 6 kinds of ions studied in this work (see Table 8) are from the literature.[40]

Using the Stokes radius of ions, the relative permittivity of membrane pores in Table 4, the relative permittivities of membrane and solution in Tables 2 and 3, the energy barrier that hydrated ions transfer into pores, ΔW_i, for three NF membranes were calculated by eqn (20), and are summarized in Table 9.

For the sake of greater clarity, the values of ΔW_i in Table 9 were plotted against the types of electrolyte in Fig. 11. It can be seen that for any kind of NF membrane, ΔW_i varies with the kinds of electrolyte. For 1 : 1 and 2 : 2 type-electrolyte solutions, ΔW_i of co- and counter-ions are close to each other, while for 1 : 2 and 2 : 1 type-electrolyte, the values of ΔW_i between the co- and counter-ions have obvious difference. This shows that the valence of ion is a crucial factor influencing ion solvation energy barrier. For the three NF membranes, the sequence of ΔW_i for electrolyte solutions is as below: 2 : 2 > 1 : 2, 2 : 1 > 1 : 1, which implies that for two kinds of electrolyte solutions, when the valence of co-ion is the same, ΔW_i with higher valence of counter-ion is larger than that of lower valence. Furthermore, ΔW_i of 2 : 2 type-electrolyte is much larger than that of 1 : 1, 1 : 2 and 2 : 1, which shows the higher ion valence results in a larger ion solvation energy barrier, thereby ions to permeate the membrane became more difficulty. Therefore, from the perspective of ion solvation energy barrier, it can be concluded that for 2 : 2 type-electrolyte with the highest ion valence in these eight kinds of electrolyte, the permeation of ion is the most difficult.

From above discussion it is clearly that the influence of ion solvation energy barrier ΔW_i on the ion permeation into different kinds of NF membranes are different. This is because there are the difference for the three membranes in structural and electrical properties which are strongly associated with interactions between membrane and electrolytes. The interaction have been extensively investigated based on the Donnan exclusion and dielectric exclusion.[41,42]

4.3 Influence of dielectric exclusion and Donnan exclusion on membrane permeation of ion

In Sections 4.2.2 and 4.2.3, concentrations of co- and counter-ions in membrane pores and the ion solvation energy barrier for three membranes in eight kinds of electrolyte solutions were calculated. On the other hand, in our previous work,[1] a model of cylindrical pores for interpreting low-frequency relaxation has been developed, according to the model surface charged density

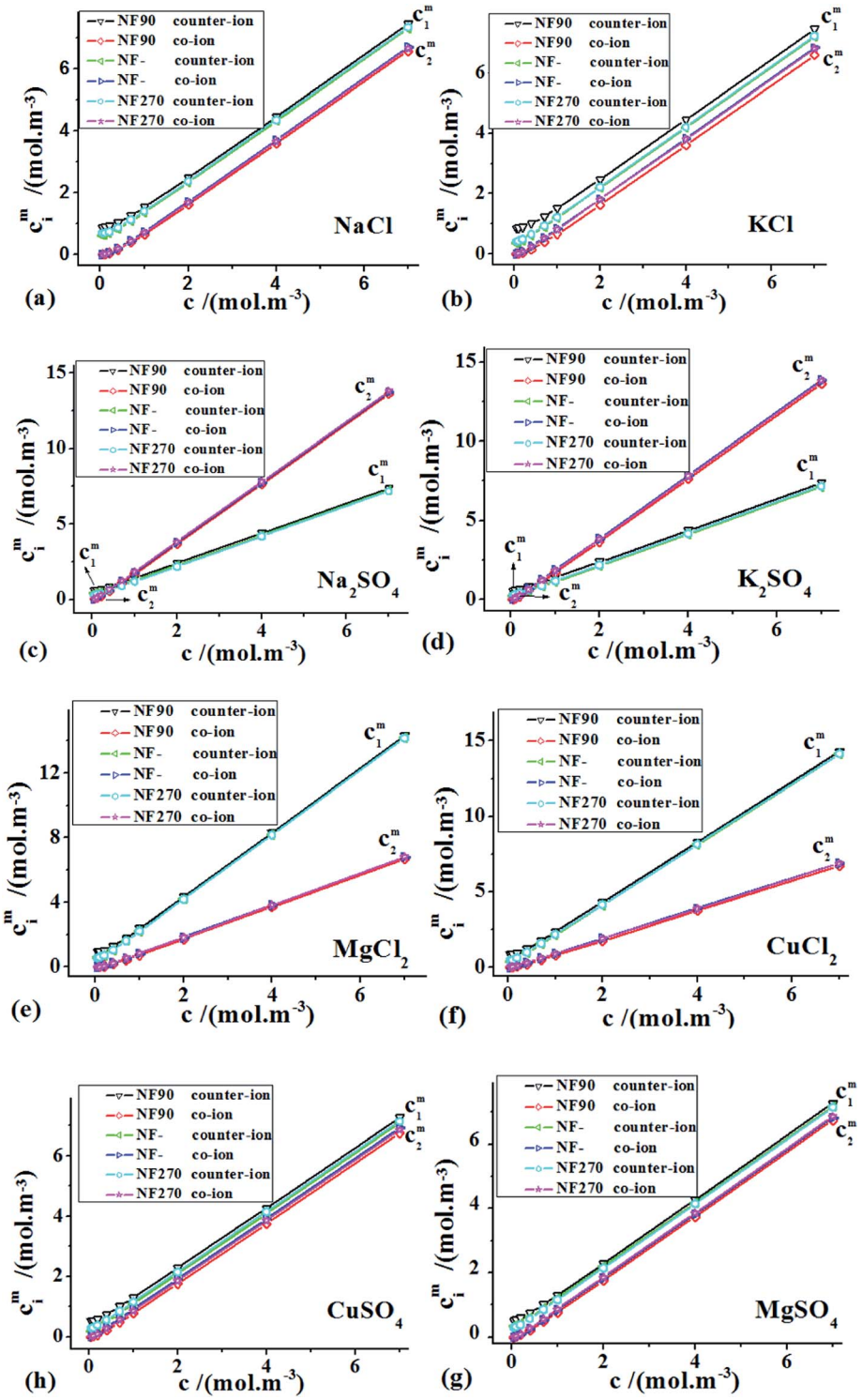

Fig. 10 Dependence of co- and counter-ion concentration c_2^m and c_1^m in membrane on solution concentration c for NF membranes in eight kinds of electrolytes.

Table 8 Stokes radius of the related ions

Ions	Na^+	K^+	Mg^{2+}	Cu^{2+}	Cl^-	SO_4^{2-}
Stokes radius r_s (nm)	0.184	0.125	0.347	0.325	0.121	0.230

σ_0 on pore-wall has been calculated. The relation between the concentrations of co-ions c_2^m and counter-ions c_1^m and charge density in pore c_{pe} can be expressed as the following expression.

$$c_{pe} = (z_1^* c_1^m - z_2^* c_2^m) \quad (21)$$

Table 9 Born solvation energy barrier of the ions between eight kinds of electrolyte solutions and NF membranes calculated from eqn (20)

		NaCl		KCl		$MgCl_2$		$CuCl_2$		Na_2SO_4		K_2SO_4		$MgSO_4$		$CuSO_4$	
Membranes	Electrolyte	Na^+	Cl^-	K^+	Cl^-	Mg^{2+}	Cl^-	Cu^{2+}	Cl^-	Na^+	SO_4^{2-}	K^+	SO_4^{2-}	Mg^{2+}	SO_4^{2-}	Cu^{2+}	SO_4^{2-}
NF90	(ΔW_i ($\times 10^{-20}$ J))	6.06	6.71	5.81	6.45	27.7	8.15	28.8	8.38	7.53	29.1	8.00	28.7	29.0	39.3	33.5	42.6
NF-		9.06	13.1	8.65	12.8	22.8	13.4	21.3	12.6	7.85	25.3	12.8	30.4	16.8	25.3	17.9	24.9
NF270		7.35	10.5	7.12	10.3	13.5	9.58	13.6	8.79	5.72	18.3	9.20	22.3	13.6	19.4	12.6	17.6

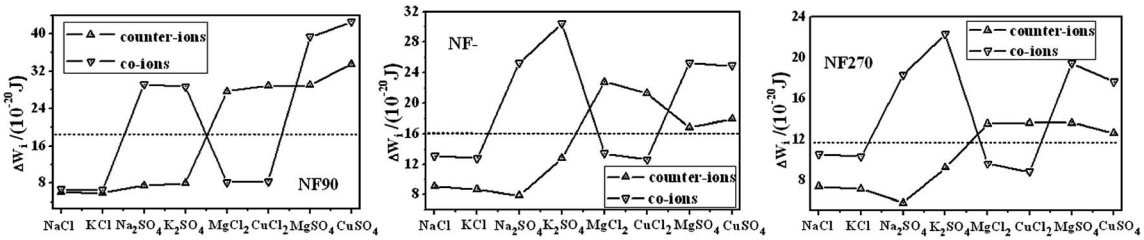

Fig. 11 Dependence of born solvation energy barrier of the counter- and co-ions between electrolyte solutions and NF membranes on kinds of electrolytes.

From this expression, it is clearly that from the view of Donnan exclusion, the larger the surface charged density σ_0 on pore-wall, the higher the charge density c_{pe} in pore should be. Therefore, by comparing c_{pe} with σ_0, the influence of Donnan exclusion on ion permeation can be clarified. That is, if the experimental results (here refers to σ_0) are in accordance with the calculated results under the consideration of Donnan exclusion (refers to c_{pe}), Donnan exclusion is dominant influence factor in ion permeation process (see 4.3.1 for a specific example). On the other hand, because ΔW_i represents the dielectric exclusion effect, in any kind of electrolyte solution, the closer the value of ΔW_i between co- and counter-ions, the lower the surface charge density σ_0 on pore-wall. Therefore, by comparing the level of similarity of ΔW_i between co- and counter-ions with σ_0, we can estimate the influence of dielectric exclusion on ion permeation of membrane. That is, if σ_0 obtained experimentally can correspond to ΔW_i, solvation energy barrier will reflect the ion permeation. In a word, on the base of σ_0, c_{pe} and ΔW_i, the dominating factor that affects ion separation process of the three kinds of NF membranes can be clarified.

4.3.1 NF90 membrane. The charge density c_{pe} in the pores of NF90 membrane in eight kinds of electrolytes solutions respectively with different concentrations was calculated by eqn (21) (see Fig. 12(b), Fig. 12(a) is the surface charge density σ_0 on pore-wall, which have been obtained in Part 1 (ref. 1)). It can be seen in Fig. 12(a) that σ_0 increases sharply at lower concentrations, and then gradually approaches to stable value as concentration increases. In addition, at lower concentrations, σ_0 in different electrolytes follow the trend: 2 : 1–2 : 2 > 1 : 2–1 : 1, while when concentration rises, σ_0 follow the trend: 2 : 1 > 1 : 2 > 1 : 1–2 : 2. In contrast, the charge density c_{pe} remain virtually unchanged in experimental concentration range. This is because electroneutrality condition were taken into account in the derivation of the ions concentration in membrane (see Section 2.2), in other words, the absolute value of c_{pe} is equal to that of membrane volumetric charge density c_e. Moreover, from Fig. 12(b), we can find that c_{pe} in different electrolyte solutions

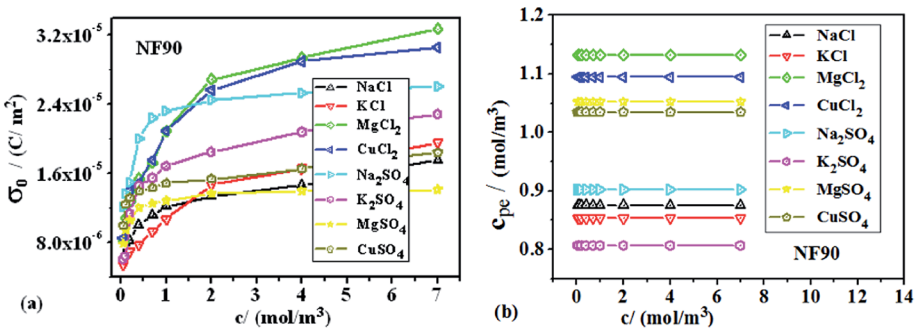

Fig. 12 The dependence of the surface charge density on the pore-wall (a) and the charge concentration in the pore (b) of NF90 membrane of eight electrolytes on the concentration of the electrolyte solutions.

follow the trend: 2 : 1 > 2 : 2 > 1 : 2–1 : 1, being similar to that of σ_0 at low concentrations. This means that Donnan exclusion is dominating factor of ion permeation. Further, it can be seen from Table 9 and Fig. 11 that for NF90 membrane, the values of ΔW_i between co- and counter-ions for 1 : 1 and 2 : 2 type-electrolytes are close to each other. This suggest that σ_0 for 1 : 1 and 2 : 2 type-electrolytes are relatively small, being consistent with the order of σ_0 at high concentrations, which shows that dielectric exclusion becomes more important to membrane permeation of ion at higher concentrations.

The above result is easy to understand: according to Donnan equilibrium principle, there is particular distribution of ions in electrolyte solution and membrane with fixed charges. When the electrolyte concentration of solution is relative lower, the counter ions in solution will be attracted strongly into the pores by the fixed charges owing to Donnan potential, resulting in the electrochemical potential of ions in the solution and membrane is equal. However, when the concentration becomes higher, the fixed charges in membrane are shielded by a large number of counter ions, Donnan exclusion loses effectiveness partially, and dielectric exclusion plays a major role in ion permeation.

4.3.2 NF- membrane. Similarly, the charge density c_{pe} in the pores of NF- membrane in eight kinds of electrolyte solutions with different concentrations are shown in Fig. 13(b) (similarly σ_0 of NF-membrane in Fig. 13(a) was obtained in Part 1 (ref. 1)). The concentration dependency of σ_0 and c_{pe} is similar to that of NF90 membrane. However, in experimental concentration, the magnitude of σ_0 follows: 1 : 1 > 2 : 1 > 1 : 2 > 2 : 2; while c_{pe} of NF- membrane in different electrolytes follows: $MgCl_2$ > $MgSO_4$ > NaCl > Na_2SO_4 > $CuCl_2$ > KCl > $CuSO_4$ > K_2SO_4, which is irregular comparing with the trend of σ_0. On the other hand, in Fig. 11(b) for NF- membrane, the similarity of solvation energy of counter-ion in different electrolytes follows: 1 : 1 > 2 : 2 > 2 : 1 > 1 : 2, which is similar to the trend of σ_0. This may suggest that dielectric exclusion plays an important role in the ion permeation process of NF- membrane at low concentration, because in the case of low the membrane volumetric charge density c_e (see Table 6), Donnan exclusion is not so obvious comparing with that of NF90 membrane.

4.3.3 NF270 membrane. Fig. 14(a) and (b) are the concentration dependence of c_{pe} and σ_0 of NF270 membrane. σ_0 of NF270 follows the trend: 1 : 1–2 : 1 > 1 : 2–2 : 2, over the experimental concentration range. While c_{pe} of NF270 membrane in different electrolytes follows the irregular trend: NaCl > $MgCl_2$, $CuCl_2$, Na_2SO_4 > K_2SO_4, KCl > $CuSO_4$, $MgSO_4$, which is different with the trend of σ_0. On the other hand, for NF270 membrane from Fig. 11(c), the level of similarity of ΔW_i of counter-ion follows the trend: 2 : 2–2 : 1 > 1 : 1–1 : 2, which is different from the trend of σ_0. This result can not give a clear explanation whether Donnan exclusion or dielectric exclusion is a dominating factor of ion permeating into NF270-membrane.

Strictly speaking, the changes of salt concentrations may more or less alter the pH of the solution, and then changes the surface charge density σ_0. For this, the pH of stock solutions of

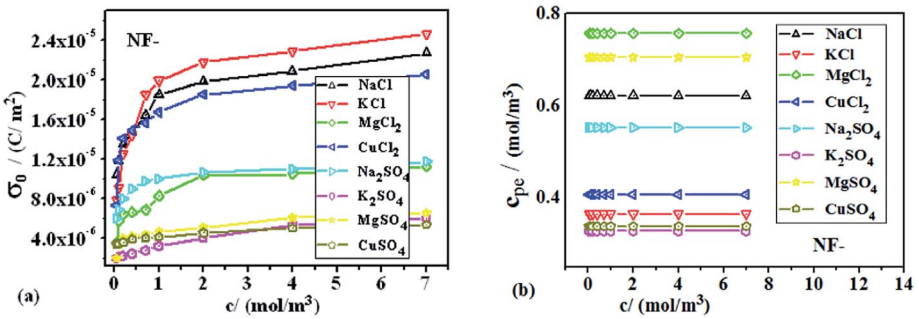

Fig. 13 Dependence of surface charge density (a) and charge concentration (b) in the pore-wall of NF- membrane on the concentration of eight electrolyte solutions.

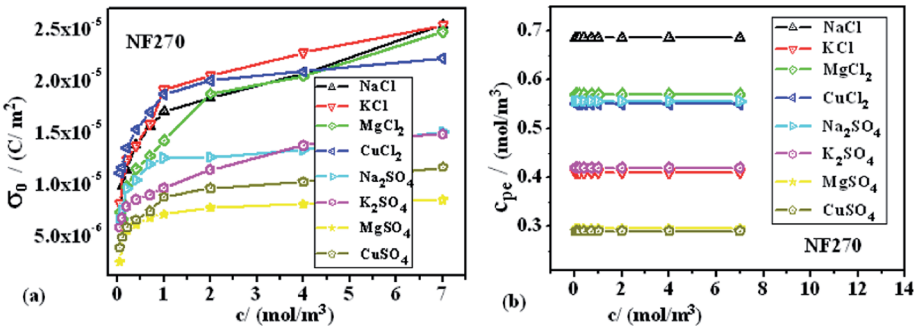

Fig. 14 Dependence of surface charge density (a) and charge concentration (b) in the pore-wall of NF270 membrane of eight electrolytes on the concentration of the electrolyte solutions.

all salts at all concentrations were measured (see the Fig. S1 of the ESI†). It is obvious that different salts and different concentrations of identical salts show biggish differences in pH values. The differences may also affect the protonation of the carboxylate groups located the pore walls, giving rise to different surface charge density. But for all this, the changing trends of σ_0 with concentrations shown in Fig. 12(a), 13(a) and 14(a) can still assess the dominating factor of Donnan exclusion in the membrane permeation of ion.

5. Concluding remarks

The conclusions of this paper include three aspects. First, on the basis of the interfacial polarization theory, the high-frequency dielectric relaxation was analyzed and relative permittivity and conductivity of membrane and solutions, ε_m,κ_m,ε_w,κ_w, were calculated. These parameters are inaccessible by any other individual experimental method. Furthermore, by discussing the variations of these parameters with concentration and species of the electrolyte, we found that ion permeation would lead to alteration of electrostatic interaction between polymer backbones of the membrane.

Secondly, the porosity of the NF membranes in wet state were calculated using ε_m, radius and thickness of the membrane. By combining κ_m/κ_w with TMS model, the membrane volumetric charge densities of the three types of membranes, which is an vital membrane parameter in research of membrane separation performance, were calculated. The expressions of concentrations of co-ions c_2^m and counter-ions c_1^m in membranes were deduced under the consideration of Donnan exclusion. Ion solvation energy barrier was calculated by using ε_m of wet membrane. The energy barriers to the solvation of ion into pores of three types of NF membranes in eight electrolytes solutions were discussed in detail, it was found that for 2 : 2 type electrolytes with the highest ion valence in these electrolyte solutions, ions permeation is the most difficult in terms of energy barrier. The all electrical parameters obtained in this work should be closer to the practical membrane process, because the relative permittivity of wet membrane was used in the calculations.

Finally, by combining the surface charge density σ_0 with concentrations of co- and counter-ions and energy barrier, the factor influencing ion separation process were suggested. From the view of Donnan exclusion, the larger the surface charge density σ_0 on pore-wall, the larger the charge density c_{pe} in pore; on the other hand, from the view of dielectric exclusion, in one kind of electrolyte solution, the closer the value of solvation energy barrier of co- and counter-ions, the lower the values σ_0. From this, main factor are clarified for each type of NF membrane. For NF90 membrane, Donnan exclusion is the dominating factor of ion permeation at low concentration, while when the concentration increases, dielectric exclusion becomes the dominating factor. For NF- and NF270 membrane, dielectric exclusion plays an important role in ion permeation of membrane over all of the experimental concentration range.

In summary, NF membranes immersed in electrolyte solutions were systematically investigated and some information on ion permeability and selectivity through membrane by analyzing dielectric spectra coupled with the transport models. Additionally, this paper may provide some enlightenments for solving the problems that are always encountered in complex membrane–solution systems. However, it should be noted that although the dielectric analyzing method proposed by us has provided a lot of information about the membrane and ion transfer process from the membrane, including some unique parameters just by analyzing the relaxation processes, the analysis procedure is still rather tedious and complex. Therefore, it is inevitable that during the analyzing processes the errors in electrical and structural parameters are brought by the computation and fitting experiment data, which may affect accurate judge to some conclusions. In addition, it is also hard to obtain these parameters simultaneously when two or more variables are requested to change, for example, like the pH and concentration in this work. Due to the above disadvantages and relative merits of the method, it will be necessary to model the studied system appropriately and lessen the variables in analyzing equations for improvement fitting precision.

Acknowledgements

Financial support of this work by the National Natural Science Foundation of China (no. 21173025, 21473012) and the Major Research Plan of NSFC (21233003) are gratefully acknowledged.

References

1 Q. Lu and K. S. Zhao, *J. Phys. Chem. B*, 2010, **114**, 16783–16791.
2 Z. G. Zhan, J. S. Xiao, D. Y. Li and M. Pan, *J. Power Sources*, 2006, **160**, 1041–1048.
3 A. E. Childress and M. Elimelech, *Environ. Sci. Technol.*, 2000, **34**, 3710–3716.
4 Y. Lanteri, P. Fievet and A. Szymczyk, *J. Colloid Interface Sci.*, 2009, **331**, 148–155.
5 W. J. Shang, X. L. Wang and Y. X. Yu, *J. Membr. Sci.*, 2006, **285**, 362–375.
6 A. Cañas, M. J. Ariza and J. Benavente, *J. Membr. Sci.*, 2001, **183**, 135–146.
7 Y. P. Zhang, T. W. Xu and R. Q. Fu, *Desalination*, 2005, **181**, 293–302.
8 J. Garcia-Aleman and J. M. Dickson, *J. Membr. Sci.*, 2004, **235**, 1–13.
9 A. Szymczyk, N. Fatin-Rouge, P. Fievet, C. Ramseyer and A. Vidonne, *J. Membr. Sci.*, 2007, **287**, 102–110.
10 A. W. Mohammad, N. Hilal, H. Al-Zoubi, N. A. Darwish and N. Ali, *Desalination*, 2007, **206**, 215–225.
11 W. Richard Bowen and J. S. Welfoot, *Chem. Eng. Sci.*, 2002, **57**, 1393–1407.
12 W. Richard Bowen and J. S. Welfoot, *Chem. Eng. Sci.*, 2002, **57**, 1121–1137.
13 J. Schaep, B. Van der Bruggen, C. Vandecasteele and D. Wilms, *Sep. Purif. Technol.*, 1998, **14**, 155–162.
14 F. F. Zha, H. G. L. Coster and A. G. Fane, *J. Membr. Sci.*, 1994, **93**, 255–271.

15 H. G. L. Coster, K. J. Kim, K. Dahlan, J. R. Smith and C. J. D. Fell, *J. Membr. Sci.*, 1992, **66**, 19–26.
16 J. M. Kavanagh, S. Hussain, T. C. Chilcott and H. G. L. Coster, *Desalination*, 2009, **236**, 187–193.
17 J. S. Park, T. C. Chilcott, H. G. L. Coster and S. H. Moon, *J. Membr. Sci.*, 2005, **246**, 137.
18 J. Benavente, X. Zhang and R. Garcia Valls, *J. Colloid Interface Sci.*, 2005, **285**, 273.
19 R. Fortunato, L. C. Branco, C. A. M. Afonso, J. Benavente and J. G. Crespo, *J. Membr. Sci.*, 2006, **270**, 42–49.
20 E. K. Zholkovskij, *J. Colloid Interface Sci.*, 1995, **169**, 267–283.
21 J. S. Park, J. H. Choi, J. J. Woo and S. H. Moon, *J. Colloid Interface Sci.*, 2006, **300**, 655–662.
22 M. Naumowicz, A. D. Petelska and Z. A. Figaszewski, *Electrochim. Acta*, 2005, **50**, 2155–2161.
23 M. J. Kelly, B. Egger, G. Fafilek, J. O. Besenhard, H. Kronberger and G. E. Nauer, *Solid State Ionics*, 2005, **176**, 2111–2114.
24 K. Kiyohara, K. S. Zhao, K. Asaka and T. Hanai, *Jpn. J. Appl. Phys., Part 1*, 1990, **29**, 1751.
25 Y. H. Li and K. S. Zhao, *J. Colloid Interface Sci.*, 2004, **276**, 68–76.
26 K. S. Zhao and Y. H. Li, *J. Phys. Chem. B*, 2006, **110**, 2755–2763.
27 K. S. Zhao and J. J. Jia, *J. Colloid Interface Sci.*, 2012, **386**, 16–27.
28 K. Asami, *Prog. Polym. Sci.*, 2002, **27**, 1617–1659.
29 K. S. Cole, *Membranes, Ions and Impulses*, University of California Press, Berkeley, CA, 1968, pp. 25–32.
30 K. Asami, *Handbook on Ultrasonic and Dielectric Characterization Techniques for Suspended Particulates*, ed. V. A. Hackley and J. Texter, The American Ceramic Society, Westerville, 1999.
31 T. S. Sørensen, *Surface Chemistry and Electrochemistry of Membranes*, New York, 1999, pp. 623–635.
32 K. S. Zhao, K. Asaka, K. Asami and T. Hanai, *Bull. Inst. Chem. Res., Kyoto Univ.*, 1989, **67**, 225–255.
33 T. Hanai, H. Z. Zhang, K. Sekine, K. Asaka and K. Asami, *Ferroelectrics*, 1988, **86**, 191–194.
34 K. Asaka, *J. Membr. Sci.*, 1990, **50**, 71–84.
35 K. Asami, A. Irimajiri, T. Hanai and N. Koizumi, *Bull. Inst. Chem. Res.,Kyoto Univ.*, 1973, **51**, 231–234.
36 T. Hanai, *Membrane*, 1989, **14**, 101–103.
37 D. R. Lide, *Handbook of Chemistry and Physics*, CRC Press, Boca Raton, FL, 66th edn, 1985, pp. 231–235.
38 A. W. Mohammad, N. Hilal, H. Al-Zoubi and N. A. Darwish, *J. Membr. Sci.*, 2007, **289**, 40–50.
39 A. Szymczyk, P. Fievet, B. Aoubiza, C. Simon and J. Pagetti, *J. Membr. Sci.*, 1999, **161**, 275.
40 G. Hagmeyer and R. Gimbel, *Desalination*, 1998, **117**, 247–256.
41 A. E. Yaroshchuk, *Sep. Purif. Technol.*, 2001, **22–23**, 143.
42 A. Szymczyk and P. Fievet, *J. Membr. Sci.*, 2005, **252**, 77.